

Supplement Figure 1

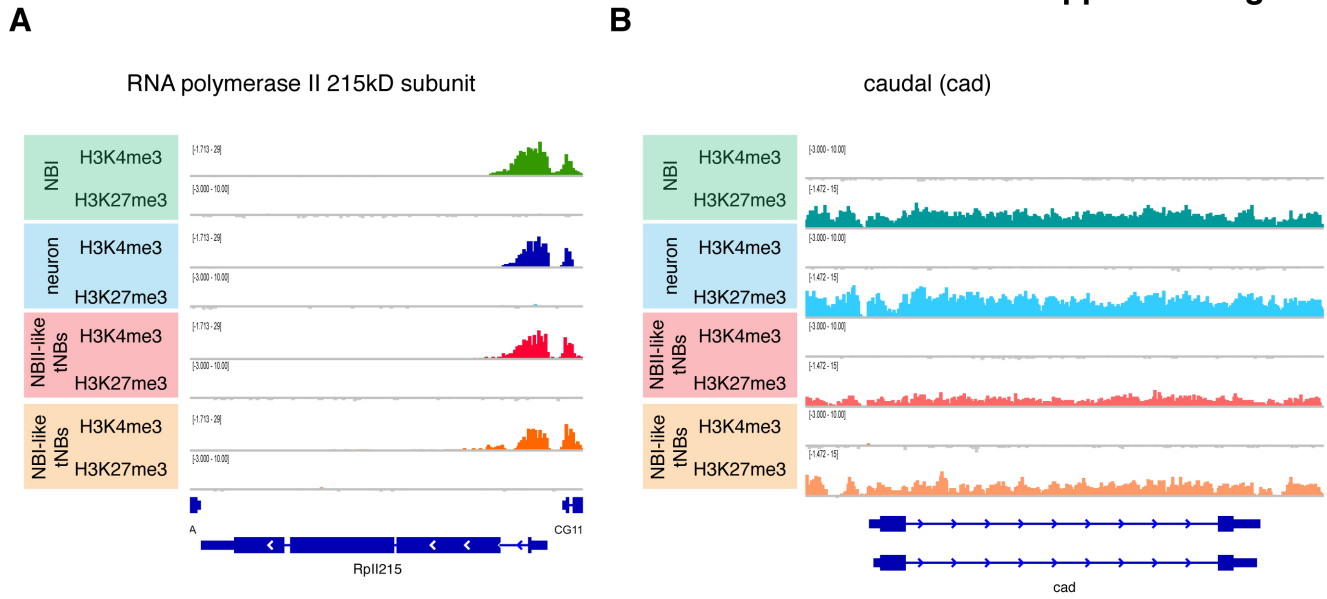


Figure S1. Examples of H3K4me3 and H3K27me3-dependent gene loci.

H3K4me3 and H3K27me3 distribution of RpLL215 (A), caudal (B).

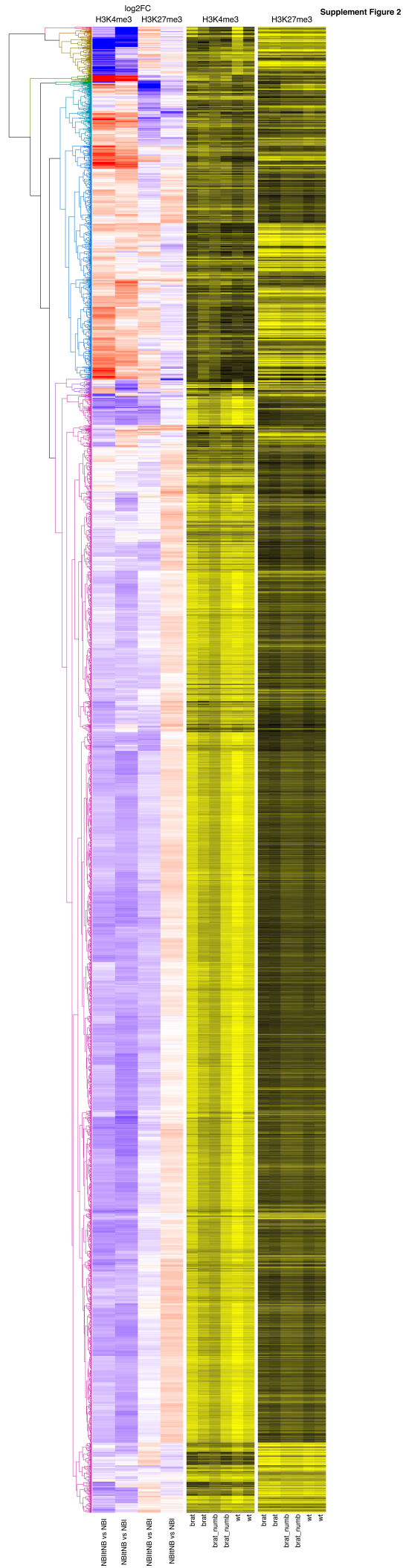


Figure S2. Full heatmap of H3K4me3 and H3K27me3 changes between NB samples.

Comprehensive hierarchical clustering analysis for NB samples presented in Figure 3.

Supplement Figure 3

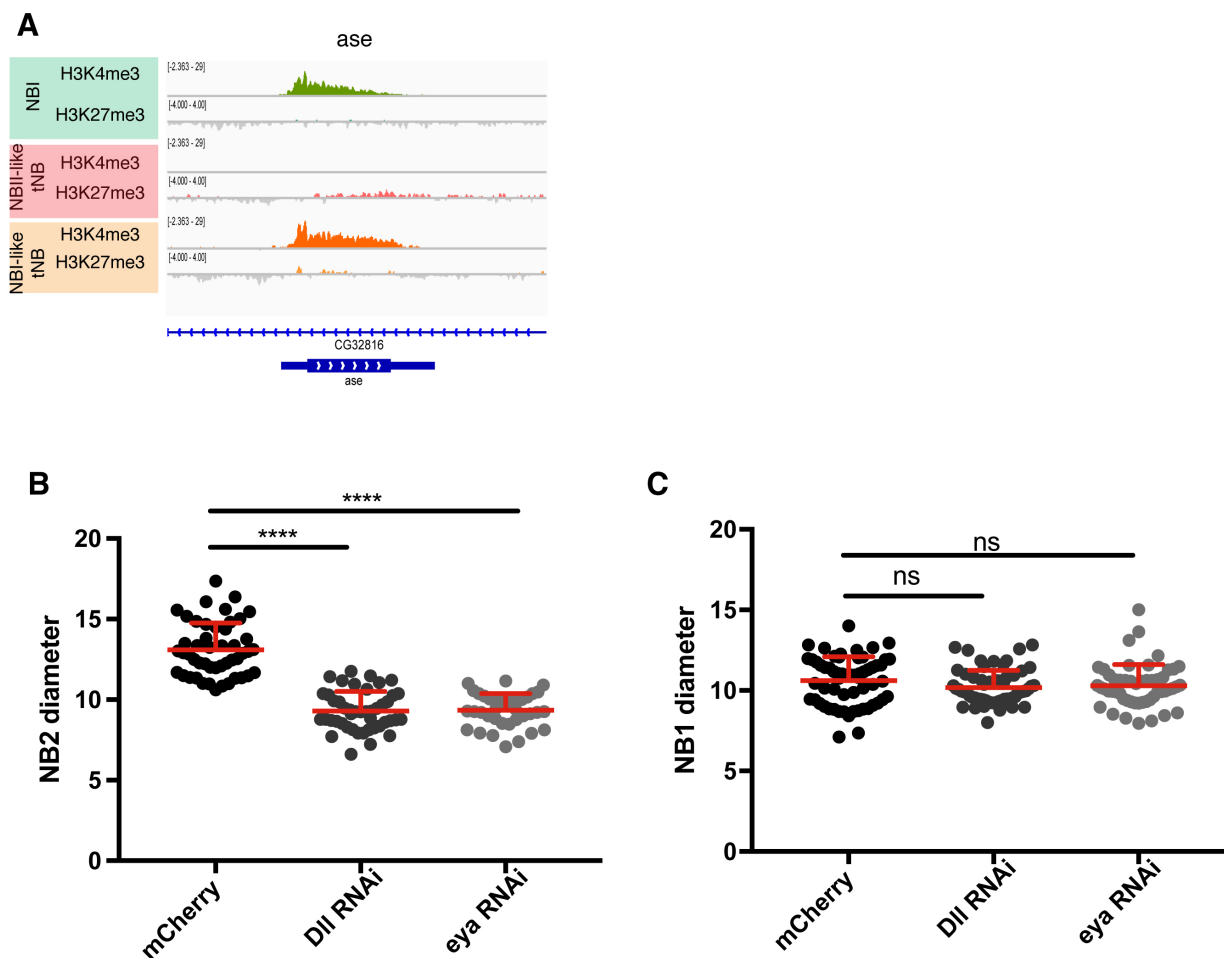


Figure S3. Dll and eya knockdown affect NBII but not NBI size.

(A) H3K4me3 and H3K27me3 distribution at the *Asense* locus. Measurements of NBII (B) and NBI (C) diameter. Driver line used was *UAS-dicer2; insc-Gal4, UAS-CD8::GFP*. Mean \pm SD is shown. (for NBII diameter (B) control = 13.09 ± 1.66 (n = 48), *Dll* = 9.29 ± 1.21 (n = 45) and *eya* = 9.34 ± 1.02 (n = 37), and for NBI diameter (C) control = 10.61 ± 1.48 (n=60), *Dll* = 10.17 ± 1.07 (n=60) and *eya* = 10.28 ± 1.33 (n=52)). One-way ANOVA test was used and ****p < 0.0001, ns = not significant. n numbers are lineages quantified.

Supplement Figure 4

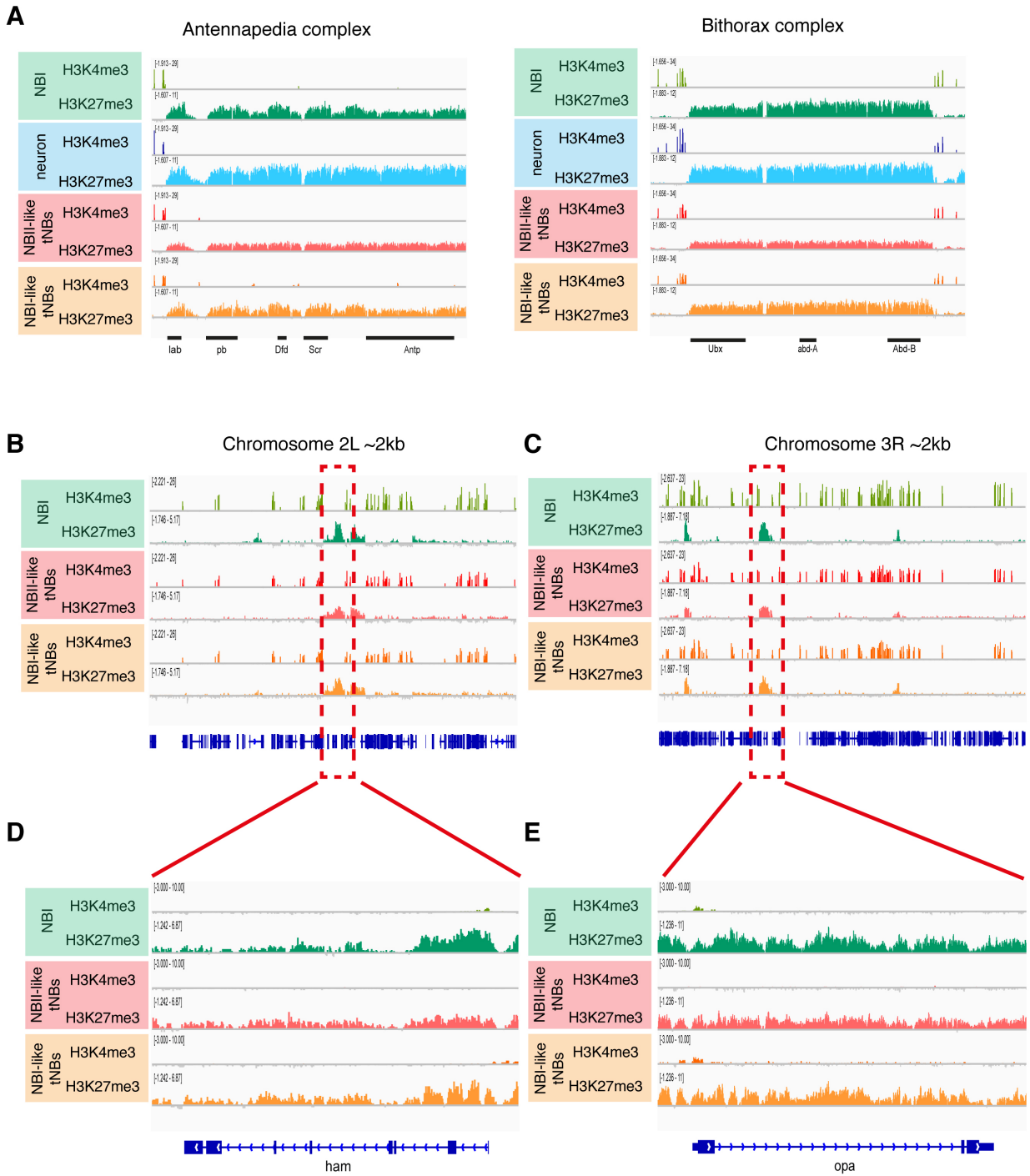


Figure S4. Examples of regions marked heavily with H3K27me3.

(A) ChIP-seq tracks of the HOX gene clusters; Antennapedia and Bithorax. H3K4me3 and H3K27me3 distribution of 2 kb region of chromosome 2L (B) and 3R (C). H3K4me3 and H3K27me3 distribution at hamlet locus on chromosome 2L (D) and odd-paired locus on chromosome 3R (E).

Supplement Figure 5

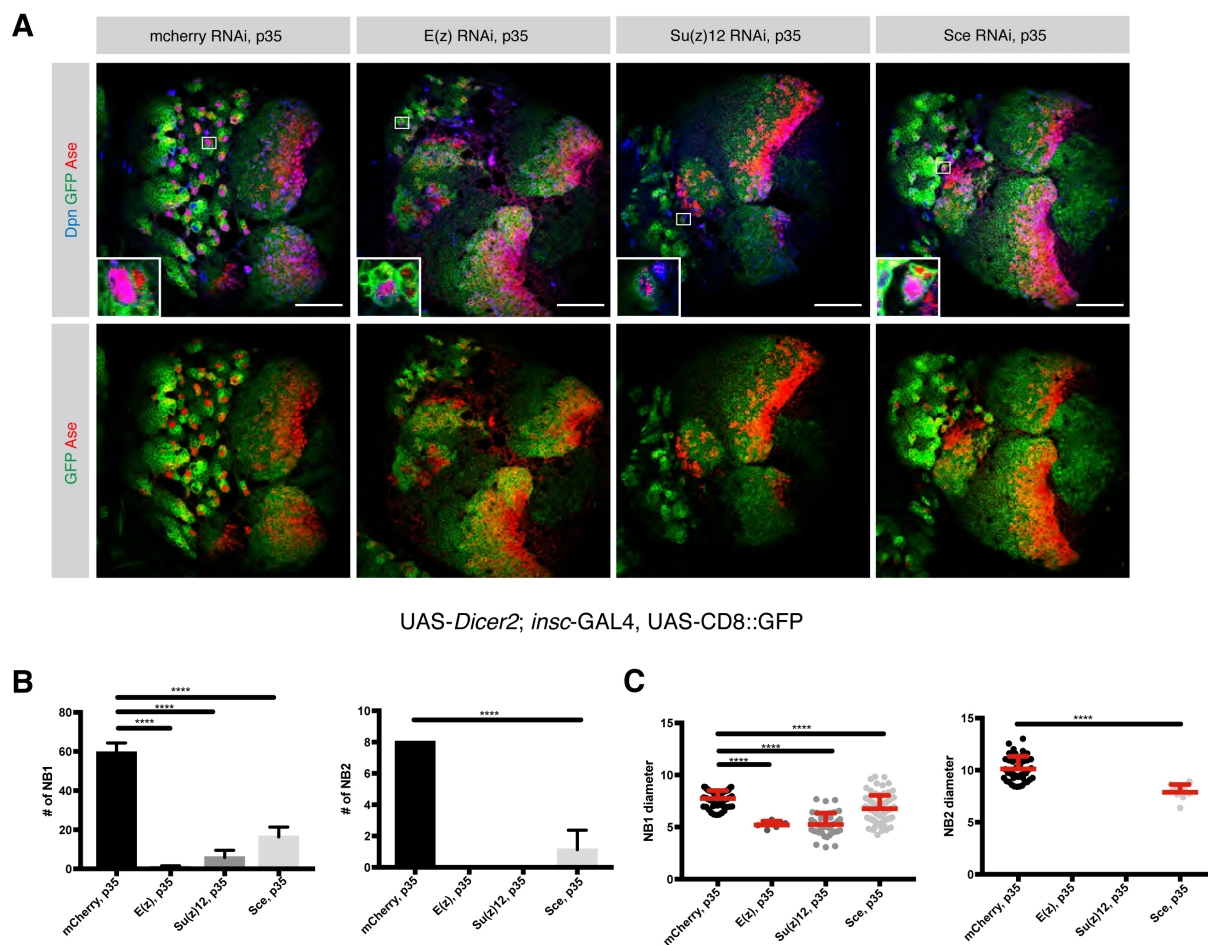


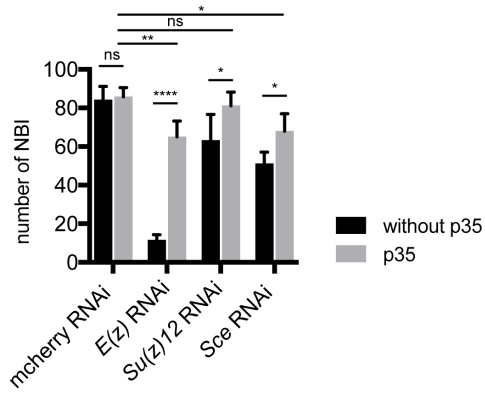
Figure S5. NBI and NBII neurogenesis depend on PcG with different sensitivity

(A) Pupal brains expressing apoptosis inhibitor P35 together with mCherry, *E(z)*, *Su(z)* and *Sce* RNAi constructs. PcG loss causes smaller NBI (blow-ups). Scale bar 50 μ m. Driver line used was UAS-*dicer2*; *insc*-Gal4, UAS-CD8::GFP.

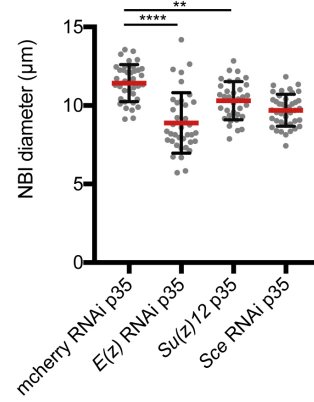
(B) Quantification of NBI and NBII numbers in (A). Mean \pm SD is shown (for NBI, mCherry+P35 = 59.43 ± 4.93 (n=7), *E(z)*+P35 = 0.62 ± 0.91 (n=8), *Su(z)12*+P35 = 5.85 ± 3.62 (n=8) and *Sce*+P35 = 16.38 ± 4.98 (n=8) and for NBII, mCherry+P35 = 8 (n=7), *E(z)*+P35 = NA, *Su(z)12*+P35 = NA and *Sce*+P35 = 1.12 ± 1.24 (n=8)). One-way ANOVA test was used and ****p < 0.0001. (C) Quantification of NBI and NBII diameter in (A). Mean \pm SD (for NBI, mCherry+P35 = 7.74 ± 0.76 (n=60), *E(z)*+P35 = 5.19 ± 0.37 (n=5), *Su(z)12*+P35 = 5.15 ± 0.92 (n=41) and *Sce*+P35 = 5.74 ± 0.82 (n=80) and for NBII, mCherry+P35 = 10.12 ± 1.2 (n=43), *E(z)*+P35 = NA, *Su(z)12*+P35 = NA and *Sce*+P35 = 7.88 ± 0.73 (n=9)) One-way ANOVA test was used and ****p < 0.0001.

Supplement Figure 6

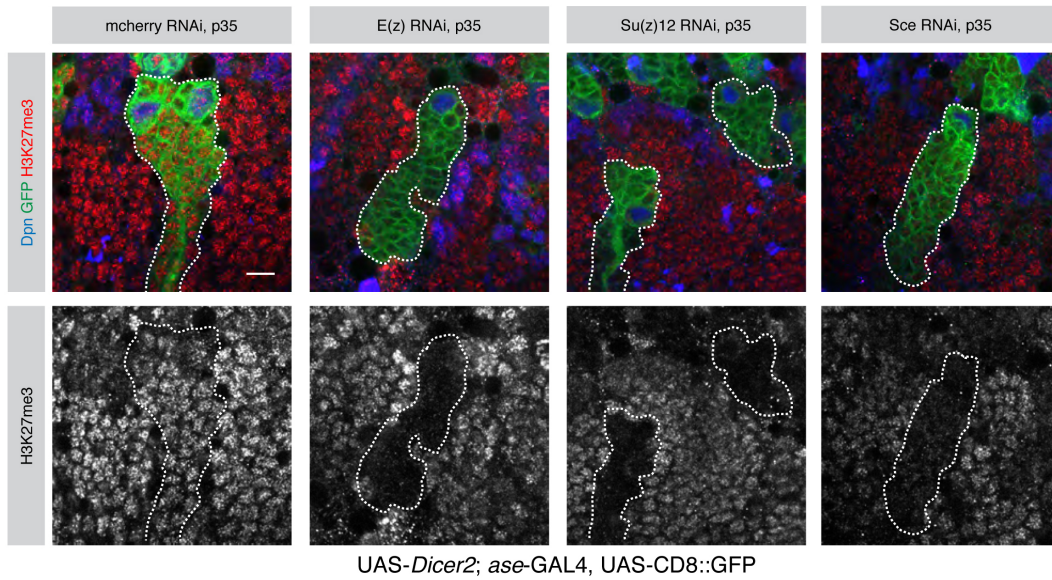
A



B



C



D

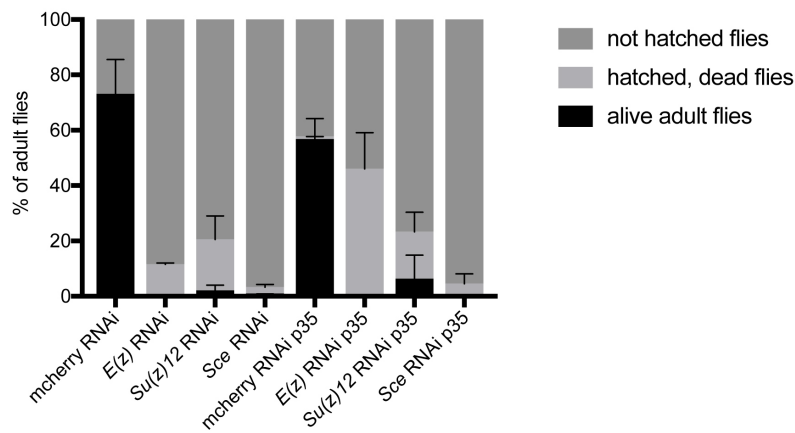


Figure S6. Blocking apoptosis in PcG depleted NB lineages does not restore neurogenesis.

(A) Number of NBI in L3 larval brains upon RNAi-depletion of PcG genes with and without blocking apoptosis with p35. Mean \pm SD. ANOVA test and * $p < 0.05$, ** $p < 0.005$, *** $p < 0.0005$, ns not significant. $n = 5$ brain lobes, except for *E(z)* RNAi and *Su(z)12* RNAi $n = 4$ brain lobes. Driver line UAS-*dicer2*; *ase-GAL4*, UAS-CD8::GFP was used. (B) Quantification of the NBI cell size of apoptosis-blocked mCherry ($n = 38$), *E(z)* ($n = 37$), *Su(z)12* ($n = 34$), *Sce* ($n = 41$) RNAi-depleted NBIs. n numbers are NBI numbers, each time from 3 different brain lobes. Driver line used was UAS-*dicer2*; *ase-GAL4*, UAS-CD8::GFP. Mean \pm SD. ANOVA test and ** $p < 0.005$, **** $p < 0.00005$. (C) H3K27me3 levels upon the knockdown of PcG genes. Exemplarily NBI lineages are outlined. Driver line used was UAS-*dicer2*; *ase-GAL4*, UAS-CD8::GFP. Scale bar $10\mu\text{m}$. (D) Quantification of adult flies that are alive, hatched but dead and did not hatch. For all conditions $n = 3$ independent viability assays. UAS-*dicer2*; *ase-GAL4*. Mean \pm SD.

Table S1: GO-term analysis of genes with decreased H3K4me3 in neurons compared to NBIs.

GO-term enrichment analysis for genes of cluster 4 (related to Fig. 2).

[Click here to Download Table S1](#)